

# An “Off-axis” Mn–Mn bond in Mn<sub>2</sub>(CO)<sub>10</sub> at high pressure†

Piero Macchi,<sup>\*a</sup> Nicola Casati,<sup>bc</sup> Shaun R. Evans,<sup>ab</sup> Fabia Gozzo,<sup>bd</sup> Petra Simoncic<sup>ab</sup> and Davide Tiana<sup>ae</sup>

Received 30th May 2014, Accepted 25th June 2014

Investigating the high pressure forms of *molecular* crystals is a relatively new field, as for many years the interest of solid state chemists and physicists was focused only on harder inorganic materials. Only a few studies were conducted before 1980,<sup>1</sup> whereas during the past decade we could witness an increasing curiosity for soft materials, in the range 0–10 GPa, with the intent to produce new polymorphs, to modify the material properties or the intra- and intermolecular bonding. Some of these studies focused on transition metal carbonyl compounds, such as M(CO)<sub>n</sub> complexes<sup>2</sup> or poly-metal species M<sub>m</sub>(CO)<sub>n</sub>.<sup>3</sup>

According to the current knowledge on transition metal dimers, high pressure should favour the smaller molecular volume (hence the lower enthalpy) of an *eclipsed* conformation, in spite of the lower electronic energy of the *staggered* one, which takes advantage of smaller repulsion between the equatorial carbonyls. Adams *et al.*<sup>4</sup> investigated the high pressure forms of transition metal carbonyl dimers M<sub>2</sub>(CO)<sub>10</sub> (M = Mn, Re) by Raman and IR spectroscopy. In Mn<sub>2</sub>(CO)<sub>10</sub> (**1**), they found a transition from *staggered* to *eclipsed* conformation (Fig. 1a and b) at 0.8 GPa, mainly justified by the reduction of the Raman C–O

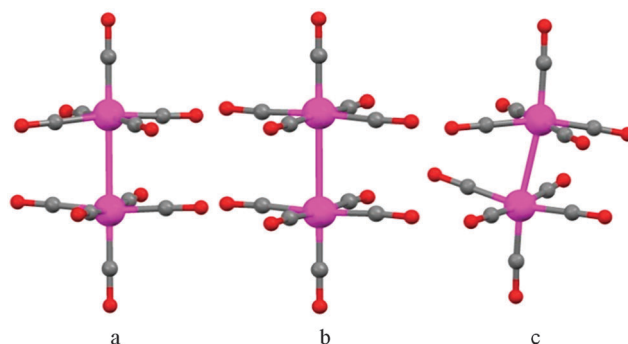


Fig. 1 (a) The stable gas phase *staggered* conformation of Mn<sub>2</sub>(CO)<sub>10</sub>; (b) the gas phase *eclipsed* conformation (proposed for the high pressure solid state form);<sup>4</sup> (c) the off-axis conformation (Mn–Mn and Mn–C<sub>axial</sub> bonds are not aligned) from P-DFT predictions and XRPD at high pressure.

stretching frequencies due to the higher symmetry. Accurate crystal structures or at least lattice parameters could not be obtained from single crystal X-ray diffraction (XRSC) analysis, because of the very fragile nature of the samples. XRSC studies and periodic density functional theory (P-DFT) calculations on other dimers, like Co<sub>2</sub>(CO)<sub>6</sub>(XPh<sub>3</sub>)<sub>2</sub>, (Ph = phenyl; X = P, As, **2a** and **2b**),<sup>5</sup> revealed a change from *staggered* to almost *eclipsed* conformation within a similar pressure range, following a second-order solid state phase transition. The interpretation of Raman spectra of M<sub>2</sub>(CO)<sub>10</sub>,<sup>4</sup> instead, suggested a sudden transformation from D<sub>4d</sub> to D<sub>4h</sub> molecular symmetry. Therefore, one would anticipate a first-order phase transition, implying discontinuous lattices.

At ambient pressure, **1** crystallizes in the *monoclinic* space group type C2/c, (reported by many authors in the non-standard I2/a). The molecular symmetry is just C<sub>2</sub>, apparently close to the gas phase D<sub>4d</sub> with a root mean square deviation of 0.19 Å. We tentatively carried out X-ray diffraction on single crystals in a diamond anvil cell (DAC), but we could only confirm the fragility of the samples. Nevertheless, two alternative investigations could be carried out: (a) P-DFT simulations using the B3PW<sup>6</sup> functional, corrected for dispersion effects,<sup>7</sup> a 6-21G(d) basis set for C and O, and a small core effective core potential

<sup>a</sup> Department of Chemistry and Biochemistry, University of Bern, Freie-strasse 3, 3012 Bern, Switzerland. E-mail: piero.macchi@dcb.unibe.ch

<sup>b</sup> Paul Scherrer Institute, Swiss Light Source, 5232 Villigen PSI, Switzerland

<sup>c</sup> Diamond Light Source Ltd., Harwell Science and Innovation Campus, Didcot, Oxfordshire, OX11 0DE, UK

<sup>d</sup> Excelsus Structural Solutions SPRL, B-1150 Brussels, Belgium

<sup>e</sup> Department of Chemistry University of Bath, UK

† Electronic supplementary information (ESI) available

**Table 1** Unit cell parameters of **1** at variable  $P$  and  $T$  conditions. More data points in ESI for experimental data, esd's are smaller than the last digit

$T$ (K)	$P$ (GPa)	$a$ (Å)	$b$ (Å)	$c$ (Å)	$\beta$ (°)	$V$ (Å <sup>3</sup> )	Ref.
298	10 <sup>-4</sup>	14.129	7.102	14.625	105.19	1417	XRPD <sup>a</sup>
298	10 <sup>-4</sup>	14.121	7.100	14.619	105.18	1414	XRPD <sup>b</sup>
298	1.55	13.816	6.647	13.735	105.00	1218	XRPD <sup>b</sup>
298	3.25	13.528	6.452	13.293	104.84	1121	XRPD <sup>b</sup>
298	6.60	13.140	6.269	12.889	104.50	1028	XRPD <sup>b</sup>
0	10 <sup>-4</sup>	14.063	6.654	13.908	108.78	1232	P-DFT
0	1.0	13.864	6.623	13.344	109.04	1158	P-DFT
0	3.0	13.338	6.493	13.016	106.97	1078	P-DFT
0	5.0	13.037	6.375	12.802	105.98	1023	P-DFT
0	10.0	12.382	6.219	12.496	103.54	935	P-DFT
298	10 <sup>-4</sup>	14.16	7.11	14.67	105.0	1426	XRSC <sup>10a</sup>
298	10 <sup>-4</sup>	14.135	7.010	14.628	105.2	1416	XRSC <sup>10b</sup>
120 <sup>c</sup>	10 <sup>-4</sup>	14.110	6.898	14.326	104.99	1347	XRSC <sup>10c</sup>
100	10 <sup>-4</sup>	14.126	6.880	14.312	105.08	1343	XRSC <sup>10d</sup>
74	10 <sup>-4</sup>	14.088	6.850	14.242	105.08	1327	XRSC <sup>10e</sup>

<sup>a</sup> Glass capillary 17 keV radiation. <sup>b</sup> Gas membrane DAC 20 keV, methanol/ethanol as a PTM. <sup>c</sup> Transformed in  $I/2a$  from the original data.

basis<sup>8</sup> for Mn; (b) X-ray powder diffraction (XRPD) in a gas membrane DAC, with a synchrotron source at the powder diffraction station of the Paul Scherer Institute.

P-DFT calculations were carried out using CRYSTAL09,<sup>9</sup> optimizing the geometry up to 15 GPa, by enthalpy minimization. Temperature effects were not included. In the range 0–3 GPa, we started from larger unit cells and a lower symmetry but the ambient condition *space group type* was always calculated as the thermodynamically stable form, of course with a smaller volume produced by a rather anisotropic compression (Table 1 and ESI†). Thus, a phase change is not predicted by the theory. Moreover, the *staggered* conformation was retained and no stationary point could be located for the *eclipsed* geometry, which rules out a conformational change without phase transition.

Two interesting geometrical changes were however calculated. One was a large contraction of the Mn–Mn bond. This is not surprising given the small force constant of this bond, but it would not occur in an *eclipsed* conformation because the repulsion between the equatorial carbonyls would force the two metals further apart, as it occurs in **2**.<sup>5</sup> The other feature was a small rotation of the Mn(CO)<sub>5</sub> moieties about an axis *perpendicular* to Mn–Mn (and parallel to the crystallographic twofold). This rotation is different from that expected for a *staggered* → *eclipsed* transformation. Thus, the Mn–Mn bond becomes “off-axis”, *i.e.* no longer aligned with the main inertial axis of the molecule. This is not only due to the external pressure, because the feature is already evident at ambient pressure. In fact, while in the gas phase  $D_{4d}$  structure, Mn–Mn, Mn–C<sub>ax</sub> and C<sub>ax</sub>–O<sub>ax</sub> bonds are co-axial (Fig. 1a), in the crystal the molecule undergoes some necessary distortions, given that  $D_{4d}$  is not a crystallographic symmetry. One of these has not been commented on so far, despite many studies on **1**, including electron density determinations:<sup>10</sup> the C<sub>ax</sub>–Mn–Mn bond angle is significantly different from 180° (see Table 2). Albeit small, this feature is important and even enhanced at high pressure: at 3 GPa, P-DFT predicts C<sub>ax</sub>–Mn–Mn = 170° and

**Table 2** Relevant geometrical parameters of Mn<sub>2</sub>(CO)<sub>10</sub> at different  $P$  and  $T$  after refinements or P-DFT optimizations. Distances are in Å; angles and torsions in °. esd's are smaller than the last digit

$T$ (K)	$P$ (GPa)	Mn–Mn	Mn–Mn–C <sub>ax</sub>	C–Mn–Mn–C <sup>a</sup>	$\epsilon^c$	Ref.
298	10 <sup>-4</sup>	2.92	178	38	0.8	XRPD <sup>b</sup>
298	1.55	2.72	168	31	1.4	XRPD <sup>b</sup>
298	3.25	2.79	170	37	7.8	XRPD <sup>b</sup>
298	6.60	2.71	166	36	12.6	XRPD <sup>b</sup>
0	10 <sup>-4</sup>	2.856	173.8	38.1	7.3	P-DFT
0	1.0	2.824	170.4	36.7	8.8	P-DFT
0	3.0	2.776	170.3	36.3	8.2	P-DFT
0	5.0	2.755	170.4	36.3	8.2	P-DFT
0	10.0	2.702	173.0	36.6	7.3	P-DFT
298	10 <sup>-4</sup>	2.92	177	38.9	n.a.	XRSC <sup>10a</sup>
298	10 <sup>-4</sup>	2.904	177.0	38.9	3.3	XRSC <sup>10b</sup>
120	10 <sup>-4</sup>	2.904	175.9	37.6	4.6	XRSC <sup>10c</sup>
100	10 <sup>-4</sup>	2.903	175.6	37.5	4.9	XRSC <sup>10d</sup>
74	10 <sup>-4</sup>	2.895	175.3	37.3	5.0	XRSC <sup>10e</sup>

<sup>a</sup> Smallest torsion angle. <sup>b</sup> DAC, 20 keV radiation, methanol/ethanol transmission medium. <sup>c</sup> Angle between the basal planes of the two Mn(CO)<sub>5</sub> pyramidal moieties (r.m.s. planes of the equatorial oxygens).

the distortion is quite evident (Fig. 1c). Above 5 GPa, the angle becomes larger (173°), but Mn–Mn still decreases. In M<sub>2</sub>(CO)<sub>*n*</sub>, M–M and M–C<sub>ax</sub> bonds are rarely constrained on the same axis by crystallographic symmetries, few exceptions are the K<sup>+</sup> salt of [Cr<sub>2</sub>(CO)<sub>10</sub>]<sup>2-</sup>, where O, C and Cr atoms lie on a twofold axis,<sup>11</sup> or species **2** where they lie on a threefold axis. [FeCr(CO)<sub>9</sub>]<sup>2-</sup>, in its PPN<sup>+</sup> salt,<sup>12</sup> is characterized by the most severe distortion (Fe–Co–C ~ 169°). In neutral molecules, the rotation is smaller (M–M–C > 175°) as for example in **1** (Table 2). Noteworthy, it is quite temperature dependent: in fact, C<sub>ax</sub>–Mn–Mn constantly decreases from 177.0(3)<sup>10b</sup> at 298 K to 175.3(1) at 74 K.<sup>10e</sup>

To prove the correctness of the theoretical predictions, we carried out high pressure powder diffraction on **1**. The species undergoes a relatively rapid decomposition under the high flux of X-ray photons, necessary to obtain significant diffraction from the very few particles loaded in the DAC. At 17 keV, a sample could not withstand more than 20 minutes of the X-ray dose, sufficient to collect a few pressure points. At higher energy, the radiation damage was smaller. The data acquisition was quite rapid thanks to the Mythen detector.<sup>13</sup> Three sets of XRPD patterns were collected: (1) 17 keV, 0–3.5 GPa, NaCl as the pressure calibrant and 4 : 1 methanol/ethanol as the pressure transmission medium (PTM); (2) 20 keV, 0–7.0 GPa, quartz as the calibrant, 4 : 1 methanol/ethanol as the PTM; and (3) 28 keV, 0–3.5 GPa, quartz as the calibrant and Daphne oil<sup>14</sup> as the PTM. After the experiments, we observed sample darkening, as previously reported,<sup>4</sup> likely due to partial decomposition. The unit cells predicted by P-DFT were used to initially index the peaks, although theoretical cells are systematically smaller because calculations are carried out at 0 K. In fact, at ambient pressure a rather large volume contraction (*ca.* 9%) is observed upon cooling from 298 K to 77 K (Table 1), thus the predicted unit cell is closer to the experimental cell at low  $T$ . The agreement between theory and experiment is better at high pressure, where the temperature has smaller influence (see ESI†). Anyway, no phase transition was observed from all

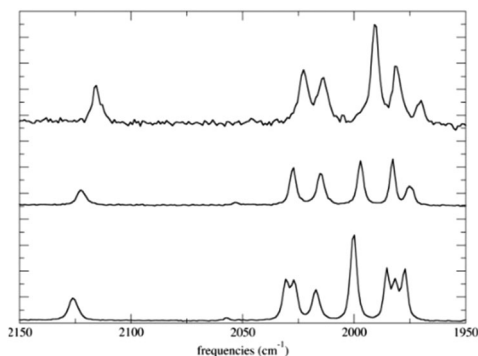


Fig. 2 Raman spectra at 0.0001 (top), 1.6 (centre) and 2.6 GPa (bottom). In Fig. 2 of ref. 4c, only three broad peaks are visible above 1 GPa in the region 1950–2050  $\text{cm}^{-1}$ . Notably, the number of predicted bands in the region 1950–2050 is even larger (see ESI†).

the data collected, proved by the  $I2/a$  phase, well explaining the positions of the observed peaks. Rietveld refinements<sup>15</sup> were carried out using TOPAS.<sup>16</sup> The  $\text{Mn}(\text{CO})_5$  unit was treated as a rigid body, allowing the rotation about the three inertial axes and translation. The results confirmed the predictions: the molecule does not modify its conformation about the Mn–Mn bond, but a substantial Mn–Mn–C<sub>ax</sub> bending occurs, as the refined angle at 3.25 GPa drops to *ca.* 170° and the basal planes of the two pyramidal  $\text{Mn}(\text{CO})_5$  moieties are quite inclined ( $\epsilon$  values in Table 2), whereas they are parallel by symmetry in the gas phase  $D_{4d}$  structure. Tentative refinements starting from the *eclipsed* conformer always converged to the *staggered* one. Although the accuracy of the refinements in DAC is small, the trend appears clear and in agreement with the calculations.

Because of the discrepancy with respect to previous results, we collected new Raman spectra on a powder sample, up to 3.0 GPa. The ambient pressure spectrum is quite similar to that previously reported by Adams *et al.*, but above 0.7 GPa there is a huge difference in the carbonyl region (1950–2050  $\text{cm}^{-1}$ ). In particular, no reduction of the number of bands is observed. This is in agreement with an unmodified, low molecular symmetry, in keeping with the P-DFT predicted spectra, after re-scaling the frequencies to account for anharmonic terms (see ESI†). The discrepancy with Adams *et al.*<sup>4</sup> could be justified by the scarce resolution of their spectra or a non-hydrostatic pressure inside the DAC that caused rather broad peaks in the region 1975–2030  $\text{cm}^{-1}$  (Fig. 2). In fact, at 2.6–2.7 GPa the FWHM is above 10  $\text{cm}^{-1}$  in ref. 4c, but much smaller in our spectra (< 5  $\text{cm}^{-1}$ ). On the other hand, there is a perfect agreement for the highest energy vibration, which is quite pressure dependent and isolated (therefore easily identified): this  $A_{1g}$  mode occurs at 2115  $\text{cm}^{-1}$  under ambient conditions and at 2125  $\text{cm}^{-1}$  at 2.6 GPa, confirming a gradient  $\Delta\nu/\Delta P \sim 4 \text{ cm}^{-1}/\text{GPa}$  (or 3  $\text{cm}^{-1}/\text{GPa}$  from P-DFT calculations).

These results prove that pressure produces two alternative effects in the  $\text{M}_2(\text{CO})_n$  species: (1) a *staggered*  $\rightarrow$  *eclipsed* transformation: the smaller molecular volume compensates the repulsion between carbonyls and the consequently longer M–M distance (it occurs in 2, with 6 equatorial carbonyls) and

(2) an approach and a slide of the  $\text{M}(\text{CO})_n$  pyramids along a OC–M–CO basal bisection together with a rotation of  $\text{M}(\text{CO})_n$  units about an axis perpendicular to M–M (it occurs in 1, where 8 equatorial carbonyls hamper the eclipsing mechanism).

To complete our study, we investigated the chemical bonding in 1 as a function of pressure, using the Interacting Quantum Atom<sup>17a</sup> analysis. The M–M interaction is associated with a small destabilization,<sup>17b</sup> a balance between a stabilizing exchange interaction (the covalent bond) and a destabilizing Coulomb interaction (the repulsion between metals that, although formally zerovalent, are positively charged due to the  $\pi$ -back donation). Upon compression, the exchange is stronger, the electron delocalization between the metals rises and the metal charges are smaller. This explains the significant Mn–Mn shortening. As known,<sup>18</sup> even for unsupported M–M bonds the equatorial carbonyls are necessary to bind the two  $\text{M}(\text{CO})_n$  moieties through 1,3-M··CO interactions. In 1, the equatorial carbonyls are more asymmetric at high pressure and one of the 1,3-M··CO interactions is particularly stabilizing. An *eclipsed* conformation would not take advantage of these two favourable effects (stronger 1,3-M··CO stabilization and smaller M–M destabilization) while having more unfavourable CO··CO contacts compared to the  $\text{M}_2(\text{CO})_8$  species.

We presented a comprehensive structural study of the high pressure form of  $\text{Mn}_2(\text{CO})_{10}$ , known for more than 50 years, but still attracting interest for its intriguing bonding features. Contrary to previously published reports,<sup>4</sup> eclipsing of the equatorial carbonyls was not observed. Instead, a translation of the  $\text{Mn}(\text{CO})_5$  squared pyramids occurs coupled with a rotation about a direction perpendicular to the Mn–Mn bond, producing a shorter and “off-axis” Mn–Mn bond. The bonding analysis confirms that this mechanism is convenient because of a better stabilization of the Mn–Mn bond and a smaller repulsion of the equatorial carbonyls compared to the *eclipsed* conformation.

The results stimulate a re-investigation<sup>19</sup> of  $\text{Re}_2(\text{CO})_{10}$ , for which *staggered*  $\rightarrow$  *eclipsed* and *eclipsed*  $\rightarrow$  *staggered* transformations were anticipated by vibrational spectroscopy at high pressure.<sup>4c</sup>

We thank the Swiss National Science Foundation (project 144534) and PSI for financial support. Ms A. Lanza and Dr M. Fisch are thanked for their assistance during experiments.

## Notes and references

- G. J. Piermarini, A. D. Mighell, C. E. Weir and S. Block, *Science*, 1969, **165**, 1250.
- S. V. Garimella, V. Drozd and A. Durygin, *Chem. Phys. Lett.*, 2008, **454**, 242.
- C. Sleboznick, J. Zhao, R. Angel, B. E. Hanson, Y. Song, Z. Liu and R. J. Hemley, *Inorg. Chem.*, 2004, **43**, 5245.
- (a) D. M. Adams, P. D. Hatton, A. C. Shaw and T. K. J. Tan, *J. Chem. Soc., Chem. Commun.*, 1981, 226; (b) D. M. Adams and I. O. C. Ekejiuba, *J. Chem. Phys.*, 1983, **78**, 5408; (c) D. M. Adams, P. D. Hatton and A. C. Shaw, *J. Phys.: Condens. Matter*, 1991, **3**, 6145.
- (a) N. Casati, P. Macchi and A. Sironi, *Chem. – Eur. J.*, 2009, **15**, 4446; (b) N. Casati, P. Macchi and A. Sironi, *Angew. Chem.*, 2005, **44**, 7736.
- (a) A. D. Becke, *J. Chem. Phys.*, 1993, **98**, 5648; (b) J. P. Perdew, *Electronic structure of solids*, Akademie Verlag, Berlin, 1991.
- S. Grimme, *J. Comput. Chem.*, 2006, **27**, 1787.
- P. J. Hay and W. R. Wadt, *J. Chem. Phys.*, 1985, **82**, 270.
- R. Dovesi, V. R. Saunders, C. Roetti, R. Orlando, C. M. Zicovich-Wilson, F. Pascale, B. Civaleri, K. Doll, N. M. Harrison, I. J. Bush, Ph. D’Arco and M. Llunell, *CRYSTAL09 User’s Manual*, University of Torino, Torino, 2009.

- 10 (a) L. F. Dahl and R. E. Rundle, *Acta Crystallogr.*, 1963, **16**, 419; (b) M. R. Churchill, K. N. Amoh and H. J. Wasserman, *Inorg. Chem.*, 1981, **20**, 1609; (c) R. Bianchi, G. Gervasio and D. Marabello, *Chem. Commun.*, 1998, 1535; (d) L. J. Farrugia, P. R. Mallinson and B. Stewart, *Acta Crystallogr.*, 2003, **B59**, 234; (e) M. Martin, B. Rees and A. Mitschler, *Acta Crystallogr.*, 1982, **B38**, 6; (f) R. Bianchi, G. Gervasio and D. Marabello, *Inorg. Chem.*, 2000, **39**, 2360.
- 11 E. Hey-Hawkins and H. G. Schnering, *Chem. Ber.*, 1991, **124**, 1167.
- 12 B. Balbach, S. Baral, H. Biersack, W. A. Herrmann, J. A. Labinger, W. R. Scheidt, F. J. Timmers and M. L. Ziegler, *Organometallics*, 1988, **7**, 325.
- 13 A. Bergamaschi, A. Cervellino, R. Dinapoli, F. Gozzo, B. Henrich, I. Johnson, P. Philipp, A. Mozzanica, B. Schmitt and X. T. Xintian, *J. Synchrotron Radiat.*, 2010, **17**, 653.
- 14 K. Yokogawa, K. Murata, H. Yoshino and S. Aoyama, *J. Phys. Soc. Jpn.*, 2007, **46**, 3636.
- 15 H. M. Rietveld, *J. Appl. Crystallogr.*, 1968, **2**, 65.
- 16 A. A. Coelho, *TOPAS-Academic*, Coelho Software, Brisbane.
- 17 (a) M. A. Blanco, A. Martín Pendás and E. Francisco, *J. Chem. Theory Comput.*, 2005, **1**, 1096; (b) D. Tiana, E. Francisco, P. Macchi, A. Sironi and A. Martín Pendás, to be submitted.
- 18 (a) P. Macchi, D. M. Proserpio and A. Sironi, *J. Am. Chem. Soc.*, 1998, **120**, 13429; (b) P. Macchi, L. Garlaschelli and A. Sironi, *J. Am. Chem. Soc.*, 2002, **124**, 141173; (c) P. Macchi and A. Sironi, *Coord. Chem. Rev.*, 2003, **238–239**, 383; (d) P. Macchi, D. Donghi and A. Sironi, *J. Am. Chem. Soc.*, 2005, **127**, 16494.
- 19 S. R. Evans, F. Flagiello, N. Casati, L. Quaroni and P. Macchi, in progress.